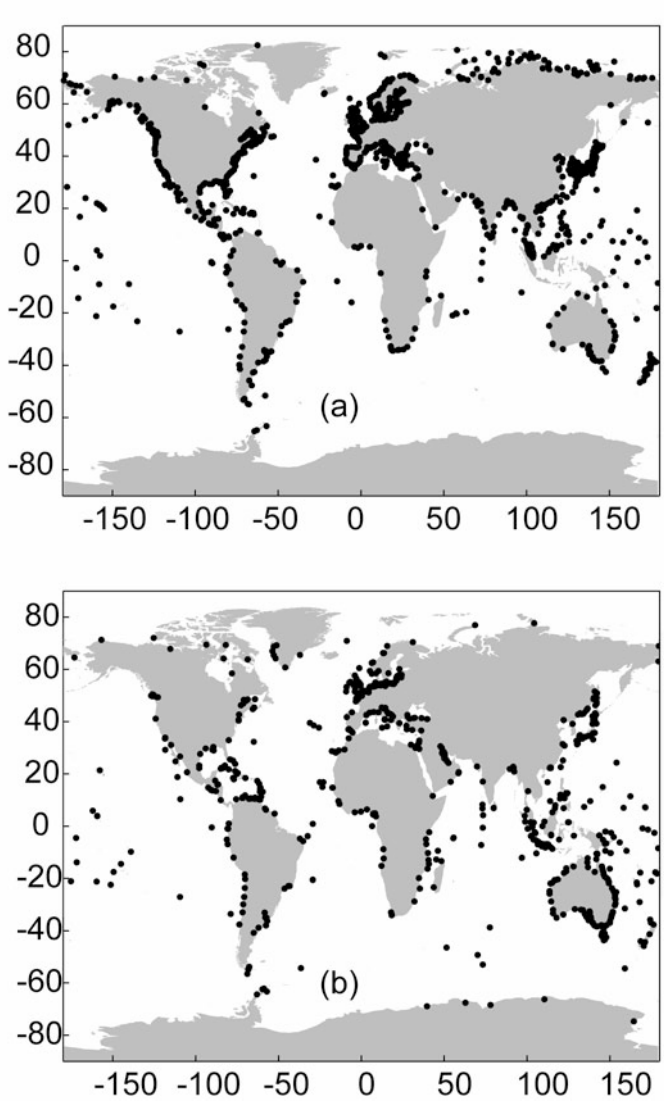

Figure 1 Positions of all tide gauges from Permanent Service for Mean Sea Level (PSMSL) dataset containing only RLR data (a) and METRIC (b) as of 24 January 2005. There are 1265 RLR and 893 METRIC tide gauges.

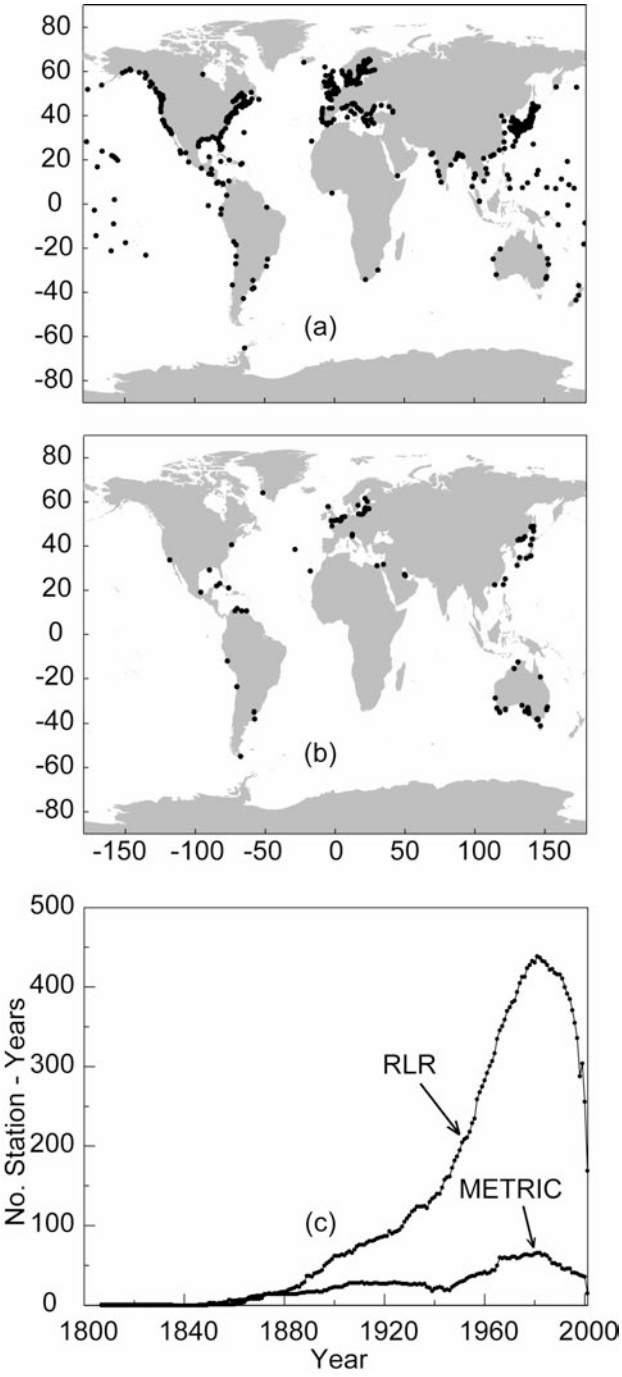

Figure 2 The locations of tide gauges with records from the PSMSL data base (as for 8/5/2003) that are longer than 20 years which were quality checked. RLR (a) contains 503 stations and METRIC (b) contains 93 stations. Within the METRIC dataset there were 12 stations that contain RLR data. The number of station-years (that are longer than 20 years) of data collected each year is shown in (c). However, due to data backlogs, the 1990's appear only half complete from a PSMSL perspective (Woodworth and Player, 2003).

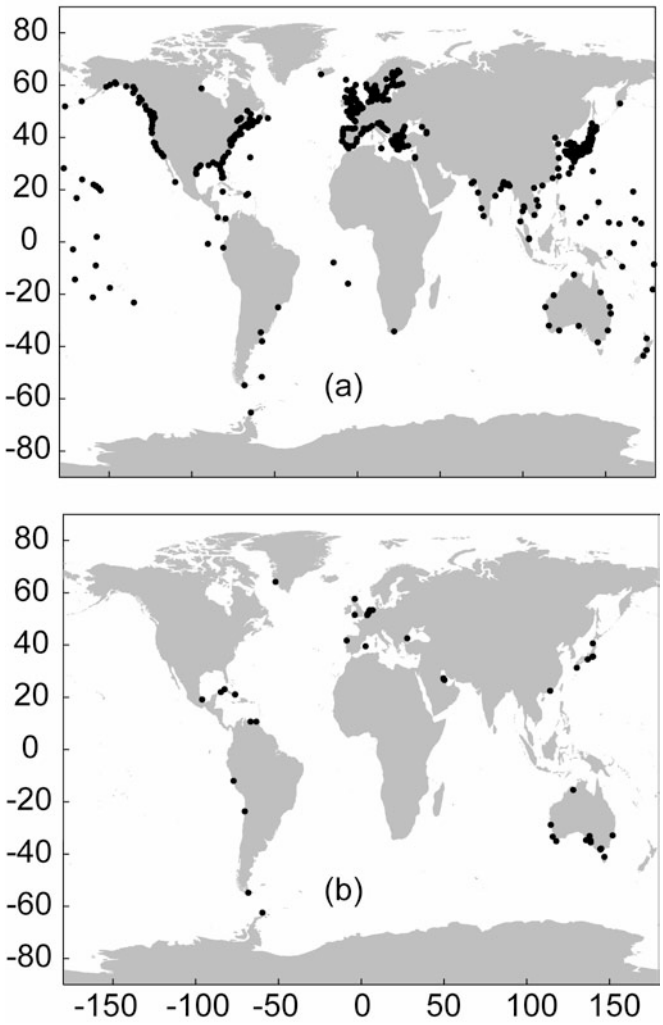

Figure 3 The locations of tide gauges with records from the PSMSL database (as for 8/5/2003) that are from 1993 were quality checked. RLR (a) contains 457 stations and METRIC (b) contains 50 stations.

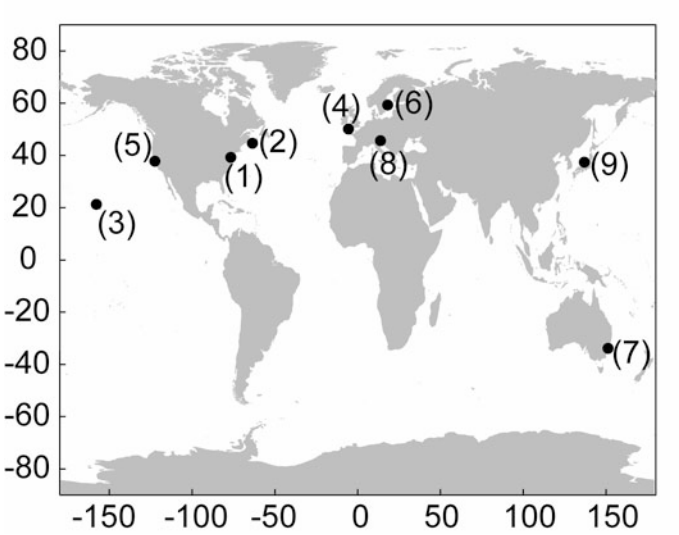

Figure 4 The location of the nine control stations used. (1) Baltimore, (2) Halifax, (3) Honolulu, (4) Newlyn, (5) San Franciso, (6) Stockholm, (7) Sydney, (8) Trieste and (9) Wajima

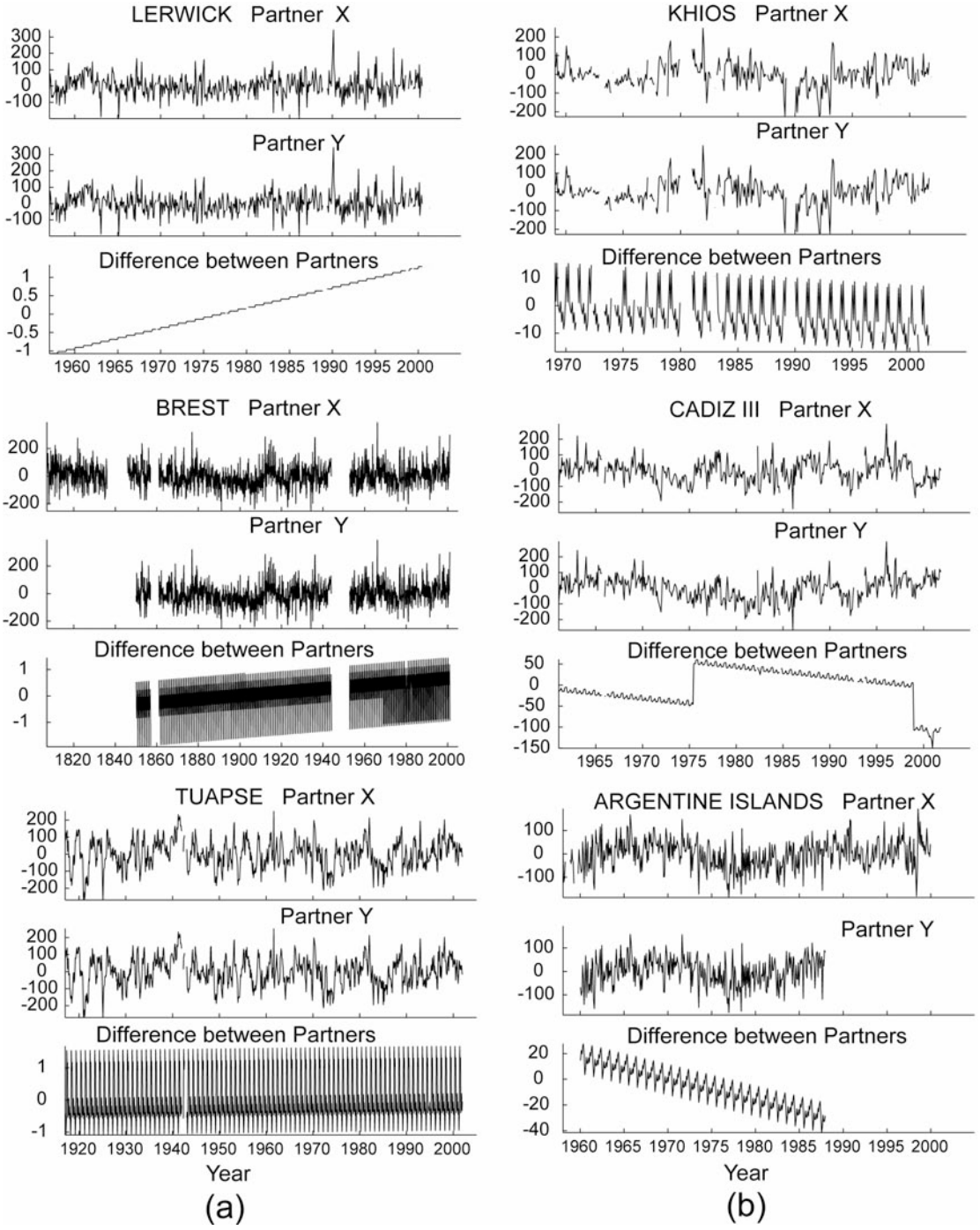

Figure 5 (a) shows examples of good comparison of the final results between partners. The y-axis is in mm. The differences in the analysis techniques are less than 3 mm where the same period of analysis is used. These results are consistent with those for the analysis of the control stations. Column (b) represents less good results due to different ways of estimating the seasonal cycle (top), or use of national dataset (middle) or use of different periods (bottom) resulting in significant differences which needed to be resolved.

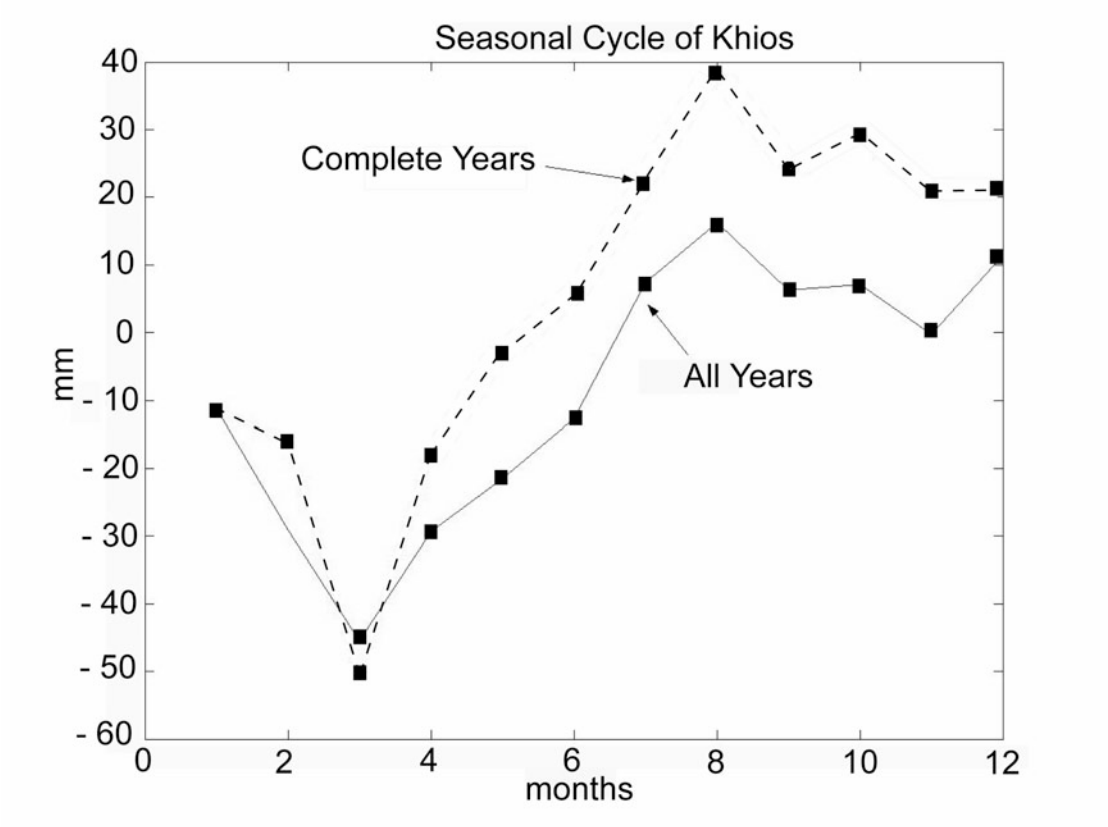

Figure 6. Mean seasonal cycle for Khios estimated from complete years only (dashed line) and for all available values (solid line). Discrepancies of up to 25 mm can occur in particular months.

Figure 7 The tide gauges with records longer than 20 years which were quality checked and analysed at SOC. The regions enclosed dote the areas for which coherency in the sea level signal was found and for which the EOF's were extracted.

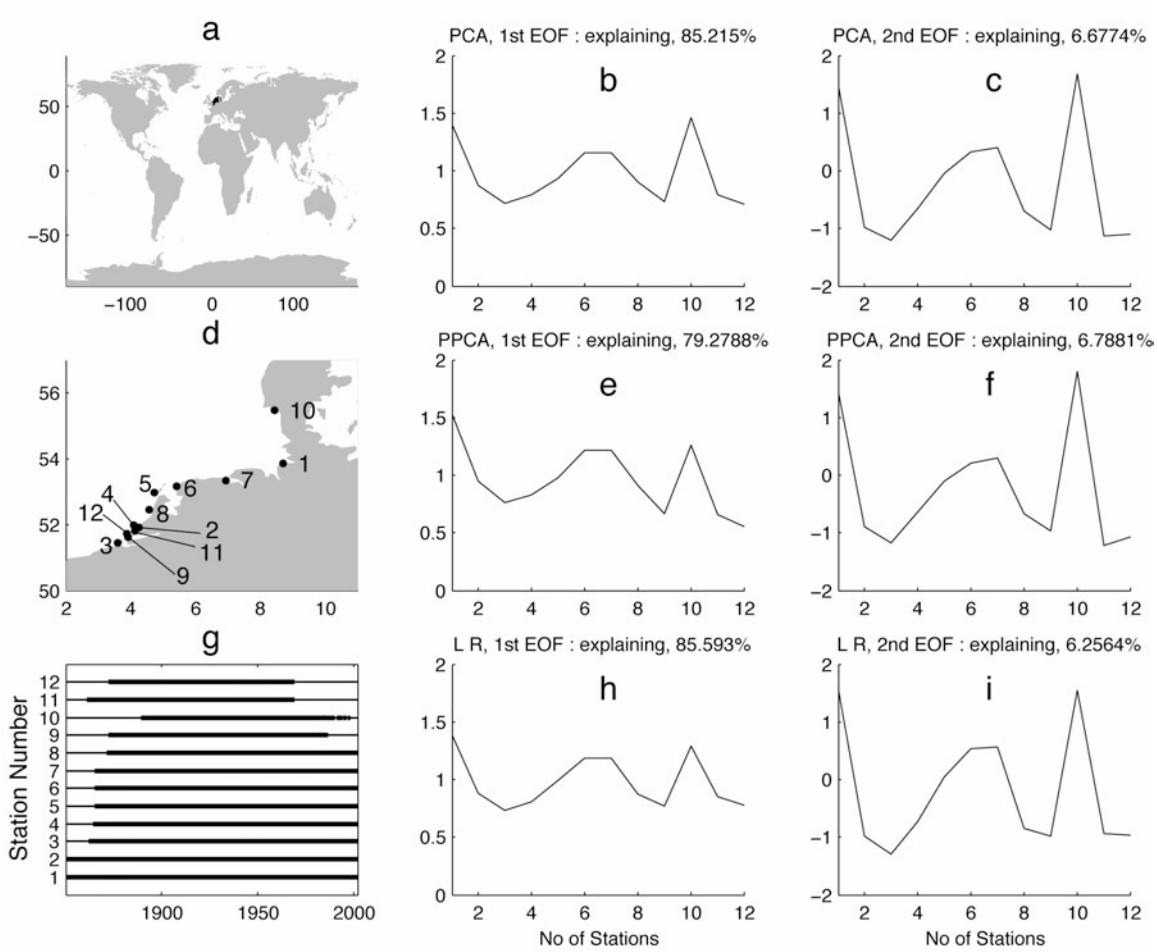

Figure 8 An example of Regional Empirical Orthogonal Functions (Southern North Sea) where there is a coherent sea level signal. The location of the tide gauge stations selected are shown a) and d). (g) The names of the tide gauge stations are as follows: Cuxhaven 2 (1), Masssluis (2), Vlissingen (3), Hoek Van Holland (4), Den Helder (5), Harlingen (6) Delfzijl (7), Ijmuiden (8), Zierikzee, (9), Esbjerg (10), Hellevoetsluis (11), Brouwershaven (12). The periods for which the selected stations have data (thin lines are interpolated data). The spatial weights of the first and second EOFs are shown in the other plots. (b) and (c) are principal component analysis (PCA) estimates; (e) and (f) are probabilistic principal component analysis (PPCA) estimates; (h) and (i) are LR estimates.

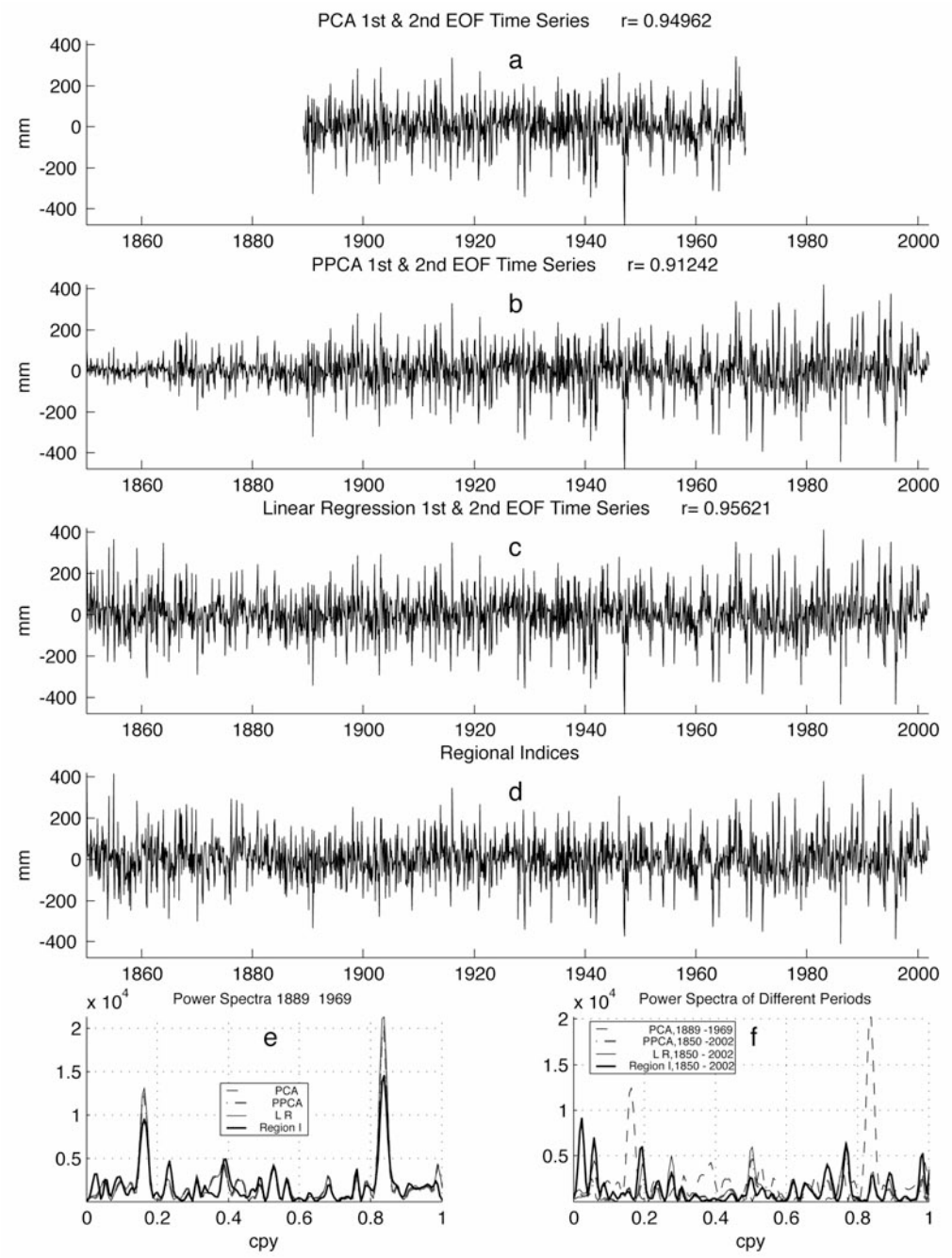

Figure 9 The time variability of the EOFs (Southern North Sea region) from (a) principal component analysis (PCA); (b) probabilistic principal component analysis (PPCA); (c) linear regression (LR). The regional index (RI) is shown at (d). The correlation coefficients are between each type of EOF and the RI. (e) shows the power spectra of (a-d) for the common period, while (f) the power spectra for the maximum period available for each of the EOF types.

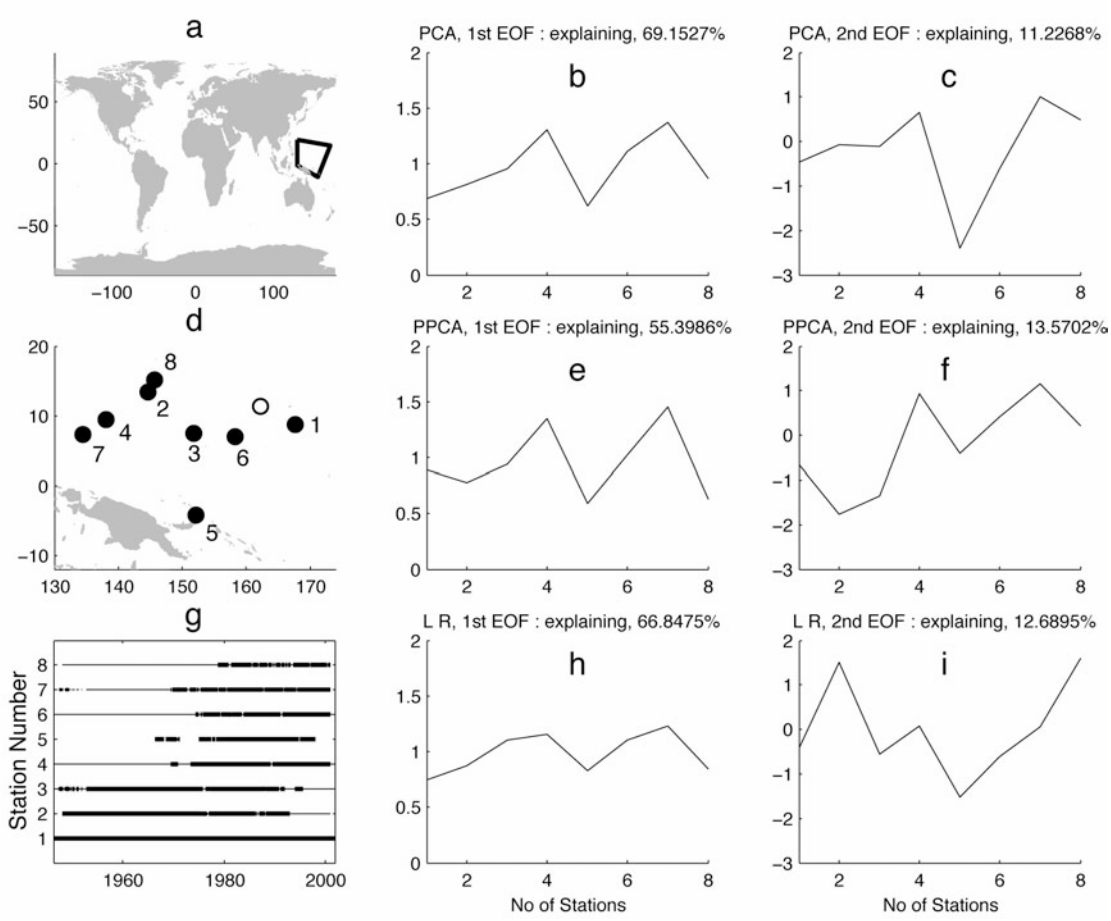

Figure 10 An example of Regional Empirical Orthogonal Functions (Western Central Pacific) where there is a coherent sea level signal. The location of the tide gauge stations selected are shown a) and d). The filled in circles are the stations that were selected which are also numbered. The circles are the stations that were not selected. (g) The names of the tide gauge stations are as follows: Kwajalein (1), Guam Chuuk (2), Moen Island (3) Yap B (4), Rabaul (5), Pohnpei-B (6) Malakal (7), Saipan (8). The periods for which the selected stations have data (thin lines are interpolated data). The spatial weights of the first and second EOFs are shown in the other plots. (b) and (c) are principal component analysis (PCA) estimates; (e) and (f) are probabilistic principal component analysis (PPCA) estimates; (h) and (i) are LR estimates.

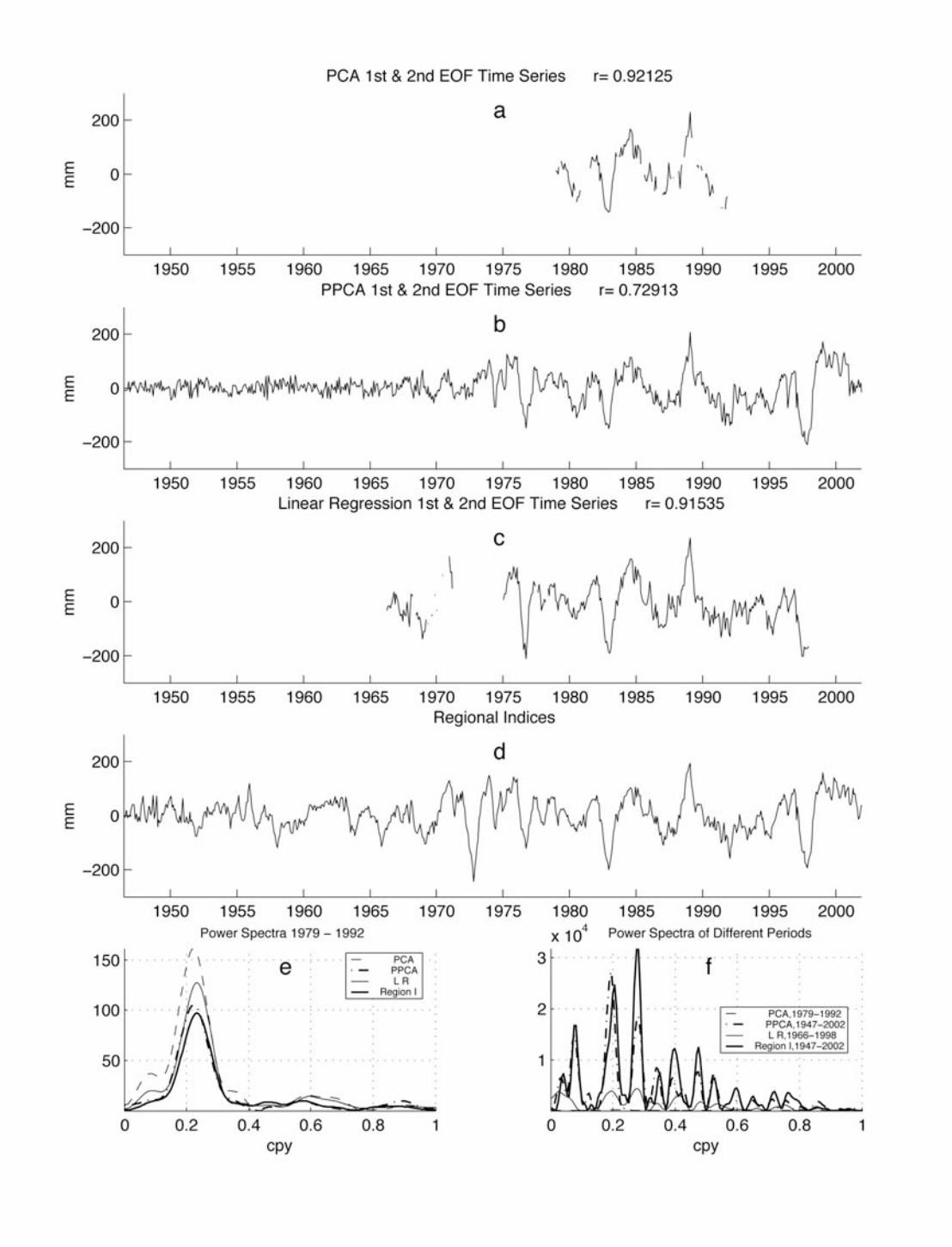

Figure 11 The time variability of the EOFs (Western Central Pacific region) from (a) principal component analysis (PCA); (b) probabilistic principal component analysis (PPCA); (c) linear regression (LR). The regional index (RI) is shown at (d). The correlation coefficients are between each type of EOF and the RI. (e) shows the power spectra of (a-d) for the common period, while (f) the power spectra for the maximum period available for each of the EOF types.